

# Using context to make gas classifiers robust to sensor drift

J. Warner,<sup>1</sup> A. Devaraj,<sup>2</sup> and R. Miikkulainen<sup>2</sup>

<sup>1</sup>*Department of Neuroscience, The University of Texas at Austin, Austin, TX*

<sup>2</sup>*Department of Computer Science, The University of Texas at Austin, Austin, TX*

The interaction of a gas particle with a metal-oxide based gas sensor changes the sensor irreversibly. The compounded changes, referred to as sensor drift, are unstable, but adaptive algorithms can sustain the accuracy of odor sensor systems. Here we focus on extending the lifetime of sensor systems without additional data acquisition by transferring knowledge from one time window to a subsequent one after drift has occurred. To support generalization across sensor states, we introduce a context-based neural network model which forms a latent representation of sensor state. We tested our models to classify samples taken from unseen subsequent time windows and discovered favorable accuracy compared to drift-naive and ensemble methods on a gas sensor array drift dataset. By reducing the effect that sensor drift has on classification accuracy, context-based models may extend the effective lifetime of gas identification systems in practical settings.

## I. INTRODUCTION

Sensor drift, defined as changes in the response properties of sensors over time, is an obstacle to the sustained accuracy of applied odor identification systems, attracting efforts to overcome it [1]. Once a sensor has been modified, one option to maintain classification performance is to recalibrate the system with new odor samples. Acquiring labeled samples is costly because it requires a skilled operator and controlled experimental conditions. Recalibrating a model with unlabeled examples, called unsupervised learning, is a promising alternative. Besides recalibration to adapt to sensor drift, a gas classifier may retain accuracy by being robust to variation. This paper focuses on extending the lifetime of sensor systems without recalibration, benchmarked by the task of generalization to unseen data recorded after sensor contamination.

The setting is a labeled dataset specifically created to demonstrate sensor drift over a period of 36 months [2]. The data is partitioned into 10 sequential classification periods, referred to as batches (Fig 1a). For each sample, there are features extracted from the responses of 16 metal-oxide based gas sensors; 8 features are calculated for each sensor, resulting in a 128-dimensional feature vector for each odor sample. The features preprocessed from the timeforms are the raw and normalized steady-state features and the exponential moving average of the increasing and decaying transients taken at three different alpha values. Six gases were presented — ammonia, acetaldehyde, acetone, ethylene, ethanol, and toluene — in arbitrary order and at variable concentrations. Sensor variability was amplified by time delays and chemical interferences presented to the sensors between batches. The dataset exemplifies sensor variance due to contamination and variable odor concentration in a controlled setting.

Industrial applications face even broader contributions to sensor variability than covered in this setting. In addition to sensor drift, which is variance due to physical modification of the sensing device, sensor variance can arise from environmental dynamics of temperature, hu-

midity, and ambient chemicals or to variability in the chemical makeup of targets odorants, sources collectively referred to as concept drift [3]. Neither does this paper cover the learning of new odor associations, part of the hard problem of unconstrained olfaction [4]. Instead, the sensor drift dataset offers a controlled testbed for sensor drift mitigation algorithms.

In this paper we follow up on previous work using ensemble methods [2] to perform generalization on this dataset. We also extend the commonly used tools of feedforward artificial neural networks (ANNs) in chemical sensor tasks [5]. Our novel method, which we call context-based learning, takes advantage of the sequential structure between batches of data in order to predict odor class accurately in the next step of the sequence. Our model has two parts: (1) a recurrent context layer, which encodes classification-relevant properties of previously seen data, and (2) a feedforward layer, which integrates the context with the current odor stimulus to generate an odor class prediction.

## II. METHODS

### A. Data preprocessing

We apply two modifications to the gas sensor array drift dataset [2], which are described below. A portion of the data with its 10-batch format is illustrated (Fig 1ab). All of the models included in this paper are constructed using our modified gas sensor array drift dataset.

The first preprocessing step is to remove all samples taken for gas 6, toluene, from the dataset. Toluene samples are absent from batches 3, 4, and 5, and this would complicate the context model. The context layer constructs its representation of the current sensor state after seeing samples of data from each odor class, so a missing gas 6 is incompatible with our architecture described. The restriction could be lifted if an unsupervised architecture is used (see Future Work).

Second, we take z-scores of features, so that all values corresponding to any given feature dimension (of the 128 total) have zero mean and variance equal to one.

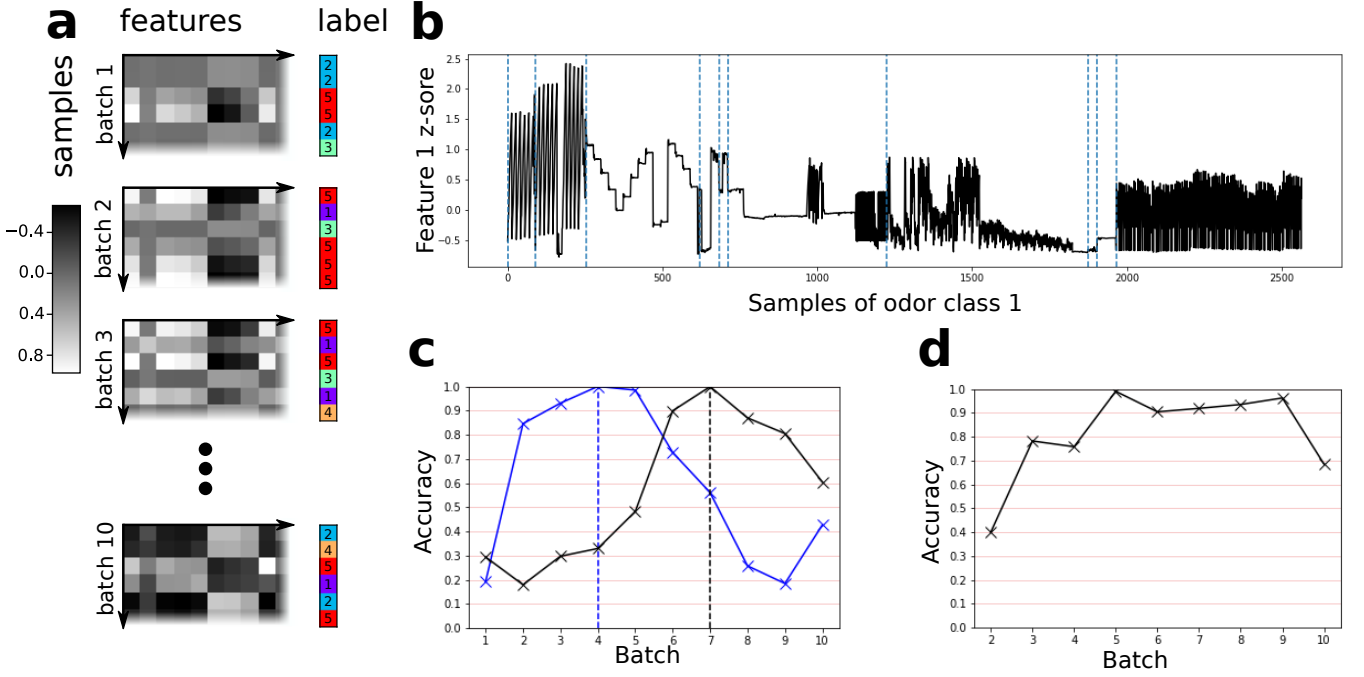


FIG. 1: **The sensor drift problem.** (a.) A sample set of feature vectors and target labels for each batch. Each sample is represented by a row of feature values represented in grayscale. Its corresponding odor class label is illustrated on the right in color. The data represents ten ordered batches of successive data collection windows. (b.) The first feature dimension is plotted for all odor samples taken of the gas ammonia. Vertical dashed lines indicate the boundaries of the different batches. (c.) Two linear discriminators obtained by linear discriminant analysis (LDA) are trained on batch 4 and on batch 7. The accuracy of the classifiers is evaluated on every batch. Note the falloff in accuracy before and after the trained batch, indicating sensor drift. (d.) To demonstrate the problem of sensor drift for classifiers, linear discriminators are fitted to all of the data from prior batches  $1, 2, \dots, T-1$  and then evaluated on the next batch  $T$ .

### B. Linear discriminant analysis

To illustrate the phenomenon of sensor drift, we include linear classifiers which are fitted to data using linear discriminant analysis (LDA) [3]. Two classifiers trained in batches 4 and 7 (Fig 1c) accurately separate the data within their batch. Performance on nearby batches is high but falls off with increasing temporal separation, revealing a sequential pattern to the sensor drift in which data becomes more dissimilar over time.

The second test introduces a train-test pattern used throughout the paper. For each batch  $T$ , a unique LDA classifier is trained using all data from batches up to but not including  $T$ . The results (Fig 1d) illustrate that batch-to-batch sensor drift degrades the accuracy of a linear classifier.

### C. Support vector machines

Some of the benchmark models use support vector machines (SVMs) with one-vs-one comparisons between all classes. SVM classifiers operate by projecting the data into a higher dimensional space using a kernel function

and then finding a linear separator in that space which gives the largest distance between the two classes being compared. Our code makes use of the Scikit-learn Python library [6], which implements its SVM classifiers using LibSVM [7]. Our SVMs are configured to use a radial basis function (RBF) as a kernel. Hyperparameters  $C$  and  $\gamma$  were determined using 10-fold cross-validation over the range  $C \in \{2^{-5}, 2^{-4}, 2^{-3}, \dots, 2^{11}\}$  and  $\gamma \in \{2^{-10}, 2^{-9}, 2^{-8}, \dots, 2^6\}$ .

### D. Ensemble classifiers

We reproduce weighted ensemble SVM classifiers [2] using our modified dataset. We also implement ensembles of neural networks analogously. In either case, the ensemble is constructed by first training single-batch classifiers on each batch from 1 through  $T-1$ . Then, each model is assigned a weight equal to its classification accuracy on batch  $T-1$ , under the presumption that batch  $T$  will be the most similar to its immediately preceding batch. Finally, to classify instances from batch  $T$ , a weighted voting procedure is used. This amounts to taking the weighted sum of each classifier's class scores.

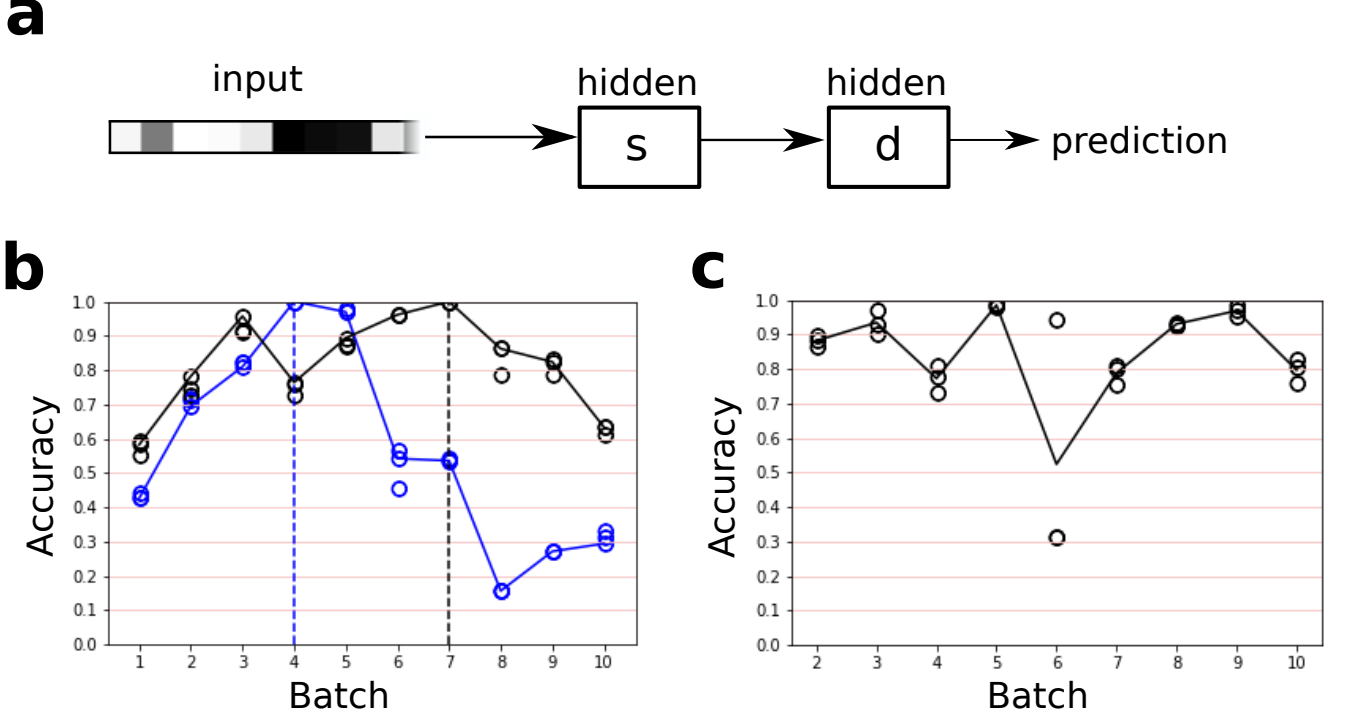


FIG. 2: **The feedforward model.** (a.) A model diagram showing an input feature vector and the two hidden layers. (b.) Feedforward networks are trained either using batch 4 (blue) and or using batch 7 (black). The accuracies when evaluated on each batch are shown. Three networks are trained on batches 4 and 7 each. The line shows the average over trials, and the circles denote the individual trials. (c.) For each batch  $T$ , networks are trained using all batches prior to  $T$ . The plot shows the average generalization accuracy when the nets are evaluated on the subsequent unseen batch  $T$ . Circles mark accuracy of each of the three trials.

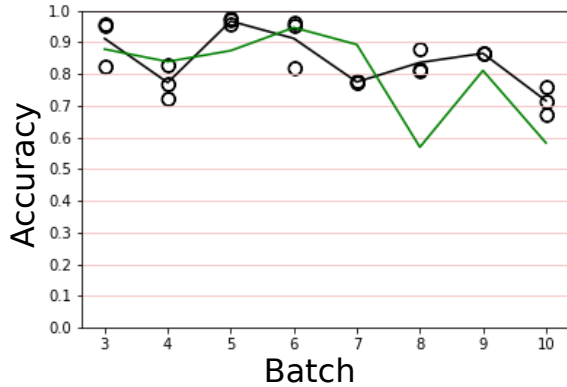


FIG. 3: **The ensemble models.** The generalization accuracy of ensemble models evaluated on batch  $T$  is plotted against the evaluation batch  $T$ . The black line represents the average over three ensembles of neural networks, with circles denoting the individual trials. The green line an ensemble of support vector machines.

### E. Artificial neural networks

The neural network code in our experiments relies on the PyTorch computing library [8], which implements automatic differentiation, enabling a neural network architecture to have an automatically computed gradient.

In the classification task, the networks are evaluated based on the similarity of their class label prediction given the target odor features to the true label (1–5). The output layer of the neural networks is a 5-dimensional vector of class scores. The value in each of component is the network’s confidence in that odor class label. The predicted class scores and true odor class are combined using the cross-entropy loss function, which is the network training signal. If  $\hat{\mathbf{y}}$  is a 5-dimensional vector representing the unnormalized model scores assigned to each class, such that  $\hat{y}_i$  represents the score the model assigned to class  $i$ , and  $c$  is the identity of the true class label, then the loss function is given:

$$\mathcal{L} = -\hat{y}_c + \log \left( \sum_i \exp(\hat{y}_i) \right)$$

All neural networks are trained using using stochastic

gradient descent with momentum [9] on the loss function  $\mathcal{L}$ . The learning rate is set to  $10^{-3}$  and the momentum factor to 0.9. No minibatching is used; instead, samples are drawn one-by-one from the training set and backpropagated through. All networks are trained for 500 epochs with a weight decay factor of  $10^{-5}$ , which prevents overfitting the model to the training data at the expense of generalization accuracy [5]. The weights of each layer are initialized to a Gaussian distribution with mean zero and variance equal to the reciprocal of the number of units in the layer. Since the initialization introduces stochasticity to training, we run each neural network experiment for three trials.

### 1. The feedforward model

The feedforward model (Fig 2a) processes odor features to compute a class prediction without explicitly handling sensor drift. The 128-dimensional feature vector,  $\mathbf{x}$ , is the input to a 50-unit skill layer,  $\mathbf{s}$ , which is connected to a 20-unit decision-making layer,  $\mathbf{d}$ , which contains a linear readout of the class scores. The model makes the faulty assumption that the training and testing sets are identically distributed, when in fact, due to sensor drift, the training and testing sets are sampled from different distributions.

The feedforward model is given as follows, where  $\mathbf{W}_{xs}$  is a  $50 \times 128$  hidden weight matrix;  $\mathbf{W}_{sd}$  is a  $20 \times 50$  hidden weight matrix; and  $\mathbf{W}_{dy}$  is a  $20 \times 5$  output matrix;  $\mathbf{b}_s$ ,  $\mathbf{b}_d$ , and  $\mathbf{b}_y$  are bias vectors of dimensions 50, 20, and 5, respectively; and ReLU is the rectified linear activation function ( $\text{ReLU}(\mathbf{x})_i = \max(0, x_i)$ ):

$$\mathbf{s} = \text{ReLU}(\mathbf{W}_{xs} \cdot \mathbf{x} + \mathbf{b}_s)$$

$$\mathbf{d} = \text{ReLU}(\mathbf{W}_{sd} \cdot \mathbf{s} + \mathbf{b}_d)$$

$$\hat{\mathbf{y}} = \mathbf{W}_{dy} \cdot \mathbf{d} + \mathbf{b}_y$$

### 2. The context model

The context model (Fig 4a) takes advantage of the sequential structure of sensor drift. Before classifying a target sample, a context layer processes a sequence of labeled context samples from the immediately preceding batches to generate a representation of the current sensor state, which we call the context vector. For evaluation, we train a unique context model for every batch  $T$ ,  $3 \leq T \leq 10$ , so that the network sees batches 1 through  $T - 1$  during training and is evaluated on its generalization accuracy on batch  $T$ . The context-based architecture consists of a recurrent context layer, a feedforward skill layer, and an integrating feedforward decision layer.

The context samples are processed in a recurrent neural network. We use long short-term memory (LSTM)

[10], a standard architecture in deep learning for its ability to learn long-range temporal associations. LSTMs regulate the flow of information through their memory via masking vectors called gates. There are two components of LSTM memory: the cell state  $\mathbf{c}_t$ , which is internal to the LSTM, and the output or “hidden” state  $\mathbf{h}_t$ , which at the end of sequence processing is exposed to the rest of the neural network.

During training, context sequences are randomly chosen from the available batches. The algorithm selects an unlabeled training sample, which is in batch  $p$ ,  $p \in \{1, 2, 3, \dots, T - 1\}$  for the network to classify. The final batch of the context sequence is  $p - 1$ , and the start batch,  $s$ , is sampled uniformly among values  $1, \dots, p - 1$ . For each batch in the context sequence, the algorithm samples  $k$  instances of each odor class. During testing on batch  $T$ , all batches 1 through  $T - 1$  are used to generate the context vector; i.e.,  $s = 1$ . We denote that  $\mathbf{x}_c^{t,z,j}$  is a feature vector from batch  $t$  of class  $z$ , and it is the  $j$ th such vector sampled. Then, the concatenation of all context samples from batch  $t$  into a single vector is named  $\mathbf{x}_c^{t,\cdot,\cdot}$ . The LSTM iteratively constructs the cell and hidden states:

$$\mathbf{c}_s, \mathbf{h}_s = \text{LSTM}(\mathbf{x}_c^{s,\cdot,\cdot}, \mathbf{0}, \mathbf{0})$$

$$\mathbf{c}_t, \mathbf{h}_t = \text{LSTM}(\mathbf{x}_c^{t,\cdot,\cdot}, \mathbf{c}_{t-1}, \mathbf{h}_{t-1})$$

The LSTM defines a series of transformations. The forget gate  $\mathbf{f}$  regulates the erasure of information, the input gate  $\mathbf{i}$  controls the flow of information from the input to the cell state, and the output gate  $\mathbf{o}$  controls the flow of information from the internal cell state  $\mathbf{c}$  to the output state  $\mathbf{h}$ . Our LSTM has 10 units, meaning that the vectors  $\mathbf{c}_t$  and  $\mathbf{h}_t$  are 10 dimensions each. Note that the context samples are ordered by their class labels, so the context samples are effectively labeled and processed by corresponding parts of the weight matrices. The LSTM equations are given:

$$\mathbf{i}_t = \sigma(\mathbf{W}_{ii} \cdot \mathbf{x}_c^{t,\cdot,\cdot} + \mathbf{b}_{ii} + \mathbf{W}_{hi} \cdot \mathbf{h}_{t-1} + \mathbf{b}_{hi})$$

$$\mathbf{f}_t = \sigma(\mathbf{W}_{if} \cdot \mathbf{x}_c^{t,\cdot,\cdot} + \mathbf{b}_{if} + \mathbf{W}_{hf} \cdot \mathbf{h}_{t-1} + \mathbf{b}_{hf})$$

$$\mathbf{g}_t = \tanh(\mathbf{W}_{ig} \cdot \mathbf{x}_c^{t,\cdot,\cdot} + \mathbf{b}_{ig} + \mathbf{W}_{hg} \cdot \mathbf{h}_{t-1} + \mathbf{b}_{hg})$$

$$\mathbf{o}_t = \sigma(\mathbf{W}_{io} \cdot \mathbf{x}_c^{t,\cdot,\cdot} + \mathbf{b}_{io} + \mathbf{W}_{ho} \cdot \mathbf{h}_{t-1} + \mathbf{b}_{ho})$$

$$\mathbf{c}_t = \mathbf{f}_t \odot \mathbf{c}_{t-1} + \mathbf{i}_t \odot \mathbf{g}_t$$

$$\mathbf{h}_t = \mathbf{o}_t \odot \tanh(\mathbf{c}_t)$$

Where  $\sigma$  is the sigmoid function, ranging from 0 to 1 and given  $\sigma(\mathbf{x})_i = \exp(x_i) / (\exp(x_i) + 1)$ , and  $\odot$  represents the Hadamard product.

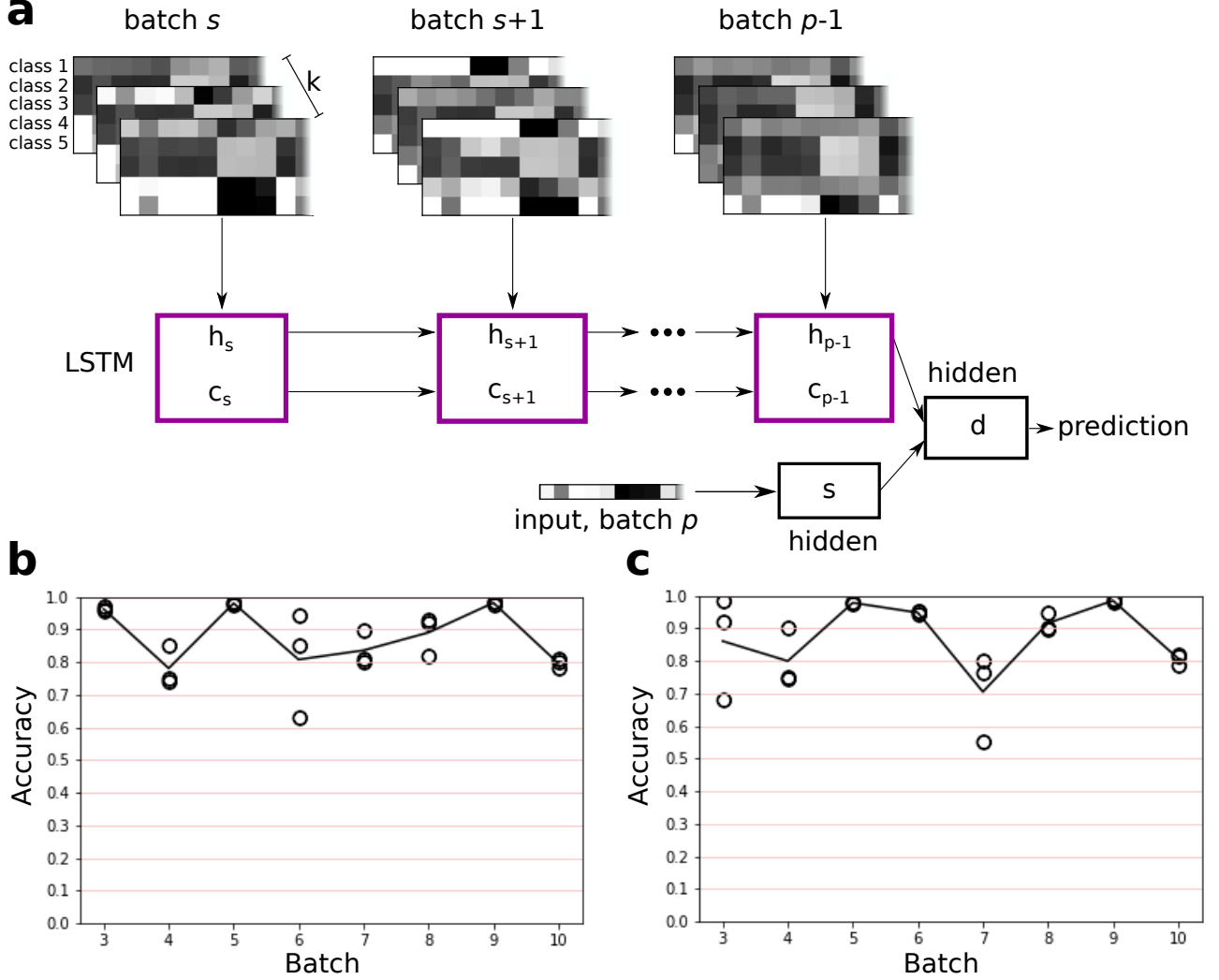


FIG. 4: **The context model.** (a.) The context model processes context samples drawn from batches  $s$  to  $p - 1$  to construct the context vector,  $h_{p-1}$ . The features corresponding to the unknown class label are processed in the skill layer  $s$ . The context layer and skill layer  $s$  are combined into a final decision-making layer  $d$  which contains a linear readout of the class predictions. The recurrent LSTM layer (purple) is shown unrolled in time; the LSTM reflects a single set of weights which is reused to iteratively refine the hidden vector  $h_t$  and cell vector  $c_t$ . (b.) The generalization accuracy of the context model. The line shows the average over three trials, and the circles denote the individual trials. (c.) The generalization accuracy of the context model with shared weights.

The output of the LSTM,  $h_{p-1}$ , is integrated with the unlabeled target sample  $\mathbf{x}$ . First, the unknown sample is processed in a 50-unit skill layer. Then, the 50-dimensional representation of  $\mathbf{x}$  and the 10-dimensional context vector are combined in a 20-unit decision-making layer which computes a linear readout of the class scores. The process is as follows:

$$\mathbf{s} = \text{ReLU}(\mathbf{W}_{xs} \cdot \mathbf{x} + \mathbf{b}_{xs})$$

$$\mathbf{d} = \text{ReLU}(\mathbf{W}_{sd} \cdot \mathbf{s} + \mathbf{b}_{sd} + \mathbf{W}_{hd} \cdot \mathbf{h}_{p-1} + \mathbf{b}_{hd})$$

$$\hat{\mathbf{y}} = \mathbf{W}_{dy} \cdot \mathbf{d} + \mathbf{b}_{dy}$$

### 3. Weight sharing

Recall the sampling procedure acquires  $k$  instances per class per batch of context. To reduce the number of parameters in our model (Table 2), we implemented weight sharing so that the same weight matrix processes all  $k$  instances. By linearity, for any matrix

$$\mathbf{W}_{i*}: \frac{1}{k} \sum_j \mathbf{W}_{i*} \cdot \mathbf{x}_c^{t,j} = \mathbf{W}_{i*} \cdot \frac{1}{k} \sum_j \mathbf{x}_c^{t,j}$$

So, implementing weight sharing is as simple as replacing in the LSTM equations the concatenation of all context in batch  $t$ ,  $\mathbf{x}_c^{t,:j}$ , with the mean,  $\mathbf{x}_c^{t,:}$ , over the  $k$  samples. Define  $\mathbf{x}_c^{t,:j}$  to be the concatenation of the  $j$ th sample in batch  $t$  of all classes. Then, the following is made the LSTM input:  $\mathbf{x}_c^{t,:} = \frac{1}{k} \sum_j \mathbf{x}_c^{t,j}$ .

Model	Batch								
	3	4	5	6	7	8	9	10	$\mu$
NN Ensemble	0.91	0.77	0.97	0.91	0.77	0.84	0.86	0.71	0.84
SVM Ensemble	0.88	<b>0.84</b>	0.87	0.95	<b>0.89</b>	0.57	0.81	0.58	0.8
NoContext	0.93	0.77	<b>0.98</b>	0.52	0.79	<b>0.93</b>	0.97	0.8	0.84
Context	<b>0.96</b>	0.78	0.98	0.81	0.84	0.89	0.98	0.8	<b>0.88</b>
ContextShare	0.86	0.8	0.98	<b>0.95</b>	0.7	0.92	<b>0.98</b>	<b>0.81</b>	0.87

TABLE I: **Generalization performance.** Listed is the classification accuracy (correct / total) of various models evaluated on the unseen testing data, batch  $T$ . The values for the neural network models represent the average accuracy over three trials. The final column represents the mean accuracy across batches 3 through 10.

### III. EXPERIMENTS

#### A. The feedforward model

We evaluate the generalization performance of feedforward artificial neural networks. We train neural networks on batches 4 and 7 and evaluate then on all batches (Fig 2b). Similar to the LDA results, the network performance degrades with the time gap between training and testing.

For each batch  $T$  from 1 to 10, we train a neural network using batches 1 through  $T - 1$ . Then, we evaluate the network’s performance on batch  $T$  (Fig 2c; Table 1, *NoContext*). The results demonstrate that, given enough data, feedforward neural networks exhibit modest generalization performance on unseen data despite sensor drift.

#### B. Ensemble models

Our second strategy is weighted ensemble methods previously reported with SVMs [2]. For each batch, from 1 to  $T - 1$ , we train three trials of neural network ensembles (Table 1, *ANN Ensemble*), and we train SVM ensembles using our 5-gas dataset (Table 1, *SVM Ensemble*). The generalization accuracies on the unseen batch  $T$  are reported.

The neural network ensemble and SVM ensembles have comparable performance (Fig 3), so we have replicated the success of previous work with ensembles and extended it to neural network ensemble models.

#### C. Context Model

We finally present results from the context model (Fig 4a). A unique context model was trained for each batch  $T \geq 3$  using batches 1 through  $T - 1$  for training.

The performance of the context model (Fig 4b; Table 1, *Context*) and the context model with weight sharing (Fig 4c; Table 1, *ContextShare*) are reported for each batch  $T$ . Of all models evaluated, models, the context-based neural network attains the highest average generalization accuracy. It scores an average generalization accuracy of

Model	Number of Parameters
NoContext	7,575
Context	136,275
ContextShare	33,875

TABLE II: **Number of parameters.** Listed is the total parameter count of the three neural network models presented.

88 percent, eliminating 26 percent of the error rate of the neural network model trained without context.

### IV. DISCUSSION

Using a gas sensor array drift dataset, we evaluate gas classifiers on their ability to generalize to unseen future data. We train feedforward neural networks, ensembles of SVMs, ensembles of neural networks, and a context-based neural network on the 5-gas odor classification task. We evaluate all models on the unseen batch subsequent to the training window. The setting is modeled on the real-world situation of having a corpus of data from previous months and then being tasked to operate on data obtained from the current unknown sensor state.

The context-based network we introduce works by extracting features from preceding sensor samples in order to estimate task-relevant sensor state. The context-based model attains the highest mean generalization accuracy in our testing. The results demonstrate that context is useful for data processing tasks. In deep learning, our method is implemented with relatively low number of layers and few hidden units per layer (Table 2). It is trainable in a number of hours on a consumer-grade CPU. By reducing the effect that sensor drift has on classification accuracy, context models may extend the effective lifetime of gas identification systems in practical settings.

### V. FUTURE WORK

The context-based network we outline relies on labeled data, so that odor samples for a given class are processed

by the appropriate part of the context layer weights. However, the algorithm is extendable to unlabeled data, simply by inputting unordered data samples to the context layer. It would be more difficult for the layer to learn sensor drift associations, since it is then faced with both variation due to drift and variation due to odor class.

The problem may be ameliorated with semi-supervised learning techniques such as self-labeled samples. If the network is made to handle unlabeled data, then it would not require instances of every class in every batch. So, the context model could be applied to the full 6-gas sensor drift dataset.

- 
- [1] Santiago Marco and Agustín Gutierrez-Galvez. Signal and Data Processing for Machine Olfaction and Chemical Sensing: A Review. *IEEE Sensors Journal*, 12(11):3189–3214, November 2012.
  - [2] Alexander Vergara, Shankar Vembu, Tuba Ayhan, Margaret A. Ryan, Margie L. Homer, and Ramón Huerta. Chemical gas sensor drift compensation using classifier ensembles. *Sensors and Actuators B: Chemical*, 166-167:320–329, May 2012.
  - [3] Saverio De Vito, Matteo Falasconi, and Matteo Pardo. Pattern Recognition. In *Essentials of Machine Olfaction and Taste*, pages 175–217. John Wiley & Sons, Ltd, 2016.
  - [4] Nabil Imam and Thomas A. Cleland. Rapid online learning and robust recall in a neuromorphic olfactory circuit. *arXiv:1906.07067 [cs, q-bio]*, June 2019. arXiv: 1906.07067.
  - [5] M. Pardo and G. Sberveglieri. Remarks on the use of multilayer perceptrons for the analysis of chemical sensor array data. *IEEE Sensors Journal*, 4(3):355–363, June 2004.
  - [6] Fabian Pedregosa, Gaël Varoquaux, Alexandre Gramfort, Vincent Michel, Bertrand Thirion, Olivier Grisel, Mathieu Blondel, Peter Prettenhofer, Ron Weiss, Vincent Dubourg, Jake Vanderplas, Alexandre Passos, David Cournapeau, Matthieu Brucher, Matthieu Perrot, and Édouard Duchesnay. Scikit-learn: Machine Learning in Python. *Journal of Machine Learning Research*, 12(Oct):2825–2830, 2011.
  - [7] Chih-Chung Chang and Chih-Jen Lin. LIBSVM: A library for support vector machines. *ACM Transactions on Intelligent Systems and Technology*, 2(3):1–27, April 2011.
  - [8] Adam Paszke, Sam Gross, Francisco Massa, Adam Lerer, James Bradbury, Gregory Chanan, Trevor Killeen, Zeming Lin, Natalia Gimelshein, Luca Antiga, Alban Desmaison, Andreas Kopf, Edward Yang, Zachary DeVito, Martin Raison, Alykhan Tejani, Sasank Chilamkurthy, Benoit Steiner, Lu Fang, Junjie Bai, and Soumith Chintala. PyTorch: An imperative style, high-performance deep learning library. In H. Wallach, H. Larochelle, A. Beygelzimer, F. Alché-Buc, E. Fox, and R. Garnett, editors, *Advances in Neural Information Processing Systems 32*, pages 8026–8037. Curran Associates, Inc., 2019.
  - [9] David E. Rumelhart, Geoffrey E. Hinton, and Ronald J. Williams. Learning representations by back-propagating errors. *Nature*, 323(6088):533–536, October 1986.
  - [10] S. Hochreiter and J. Schmidhuber. Long short-term memory. *Neural Computation*, 9(8):1735–1780, November 1997.